

## MD Simulations on the Influence of Disease-Related Amino Acid Mutations in the Human Prion Protein

Kholmirzo Kholmurodov<sup>1,2\*</sup>, Yoshinori Hirano<sup>1</sup>, and Toshikazu Ebisuzaki<sup>1</sup>

<sup>1</sup>*Advanced Computing Center, Computational Science Division, Institute of Physical and Chemical Research (RIKEN), 2-1 Hirosawa, Wako-shi, Saitama 351-0198, Japan*

<sup>2</sup>*Laboratory of Information Technologies, Joint Institute for Nuclear Research (JINR), Dubna, Moscow region, 141980, Russia*

\*E-mail: mirzo@atlas.riken.go.jp

(Received February 17, 2003; accepted May 2, 2003; published online May 31, 2003)

### Abstract

We have performed molecular dynamics simulations on the human prion protein to study the effect of point mutations in relation to the inherited form of Creutzfeldt-Jakob disease. Three model structures of the human prion protein are examined with a focus on their dynamics and conformational changes. Model 1 is an NMR structure of the globular domain (125-228) of a wild-type prion. The model consists of three  $\alpha$ -helices and an anti-parallel  $\beta$ -sheet. Models 2 and 3 are mutant structures containing a Glu200→Asp and a Glu200→Lys substitution, respectively. These models are derived from NMR structures. The Glu200→Lys mutation in model 3 is a disease-related amino acid exchange. The results of about 2-million time step calculations have shown that the globular domains of models 1 and 2 are stable, whereas, for model 3, we observe a partial unfolding and reorganization of the protein structure by insertion of the disease-related mutation Glu200→Lys.

**Key Words:** Molecular Dynamics Simulations, Proteins, Prions, Creutzfeldt-Jakob disease, Hydrogen Bond Network

**Area of Interest:** Molecular Computing

## 1. Introduction

The prion diseases, such as BSE (bovine spongiform encephalopathy), CJD (Creutzfeldt-Jakob disease), and other transmissible encephalopathies (TSE) are characterized by the transformation of a wild-type prion protein ( $\text{PrP}^{\text{C}}$ ) into a mutant, disease-related form ( $\text{PrP}^{\text{SC}}$ ) [1][2][3][4]. The familial forms of prion diseases (for example, Gerstmann-Straussler-Scheinker syndrome (GSS), fatal familial insomnia (FFI), and CJD) are known to segregate with the exchange of individual amino acids or point mutations in the prion protein sequence [5][6]. The important point is that no chemical difference between  $\text{PrP}^{\text{C}}$  and  $\text{PrP}^{\text{SC}}$  has been identified [7]. Nevertheless, experiments with circular dichroism and Fourier-transform infrared analyses have shown that  $\text{PrP}^{\text{C}}$  has a low beta-sheet content (about 3 %) and is sensitive to proteases, whereas  $\text{PrP}^{\text{SC}}$  has a high beta-sheet content (about 30 %) and is protease-resistant [8][9].

Most cases of the human prion diseases occur spontaneously with unknown causes. However, the familial prion diseases, such as GSS, FFI, and CJD, are related to distinct point mutations within the human gene of  $\text{PrP}^{\text{C}}$  [1][2][3][4][5][6]. Such point mutations are seen in the amino acid residues 102, 105, 117, 145, 198, and 217 in GSS and 178, 200, and 210 in most cases of CJD. Of particular interest is the mutation at residue 200, because this mutation is found in a well-known type of genetically transmitted CJD [5][6][7][8][9][31]. In spite of this, CJD is most often not associated with one of the specific mutations, and around 85 percent of the cases of human prion disease are sporadic [6][10][31][32][35].

The mature form of HuPrP comprises 208 residues (numbered 23-230). The C-terminal part of the polypeptide chain with residues 125-228 forms a stable, compact globular domain; whereas the N-terminal part (21-124) is unstructured in aqueous solution at pH 5 [10][11]. The C-terminal region, containing the domain 125-228, is represented by Figures 1 and 2.

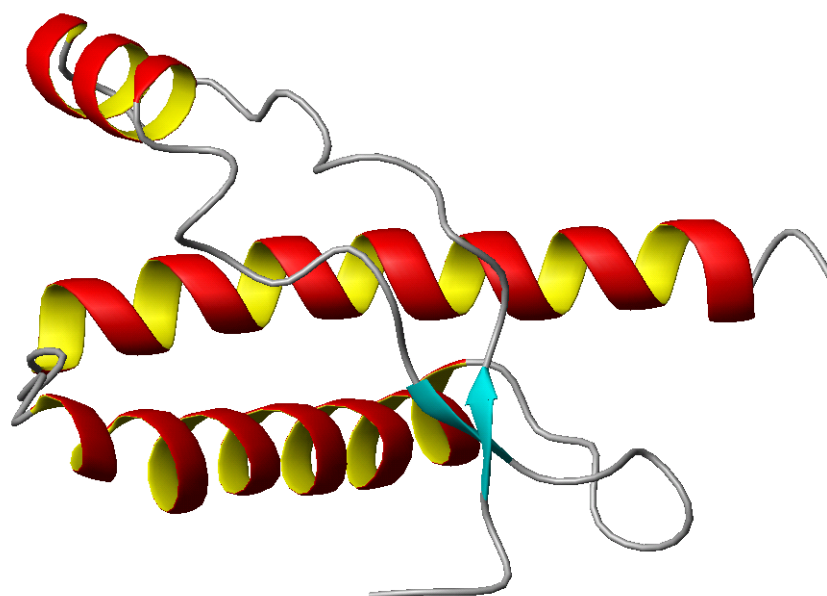


**Figure 1.** A ribbon structure of the globular domain of the HuPrP. The potential energy-minimized structure of the NMR-determined parts of HuPrP is shown

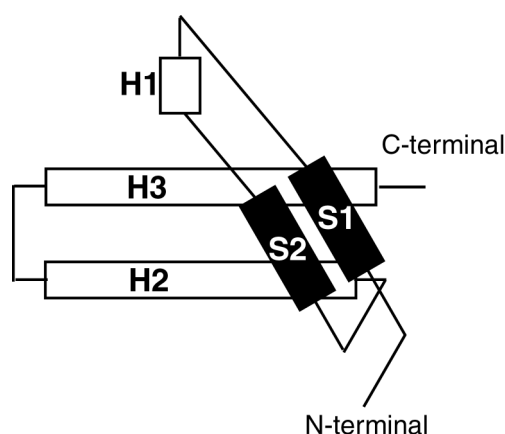


**Figure 2.** A schematic diagram of the globular domain of HuPrP. The structure consists of three  $\alpha$ -helices (H1, H2, and H3) and a short  $\beta$ -sheet (S1 and S2).

NMR experiments have recently revealed that the three-dimensional structures of the mouse prion protein (MoPrP) [11][12][13], Syrian hamster prion protein (ShPrP) [10][14][15], bovine prion protein [16], and human prion protein (HuPrP) [17] are similar, and all correspond to PrP<sup>C</sup>. These structures have indicated that the C-terminal (with residues 125-228) forms a globular domain, consisting of three  $\alpha$ -helices and a short anti-parallel  $\beta$ -sheet, whereas the N-terminal is flexibly disordered in solution. The role of the flexible N-terminal segment is not yet understood [18]. Experiments with transgenic mice, for example, suggest that the N-terminal tail specifically interacts with a ligand and may be required for signal transduction [18][19]. It is also known that the first and shortest  $\alpha$ -helix H1, which is connected to the flexible N-terminal via a  $\beta$ -strand, is hydrophilic and that other parts of the globular domain are very hydrophobic, which makes the interaction between them weak [20][21]. Experiments with a monoclonal antibody performed by Korth et al. showed that the structures of the first  $\alpha$ -helix H1 in PrP<sup>C</sup> and in PrP<sup>SC</sup> are different [22].

In the present study, we examine the correlations between the mutation at residue 200 and the related protein structures by using MD simulations. To elucidate some of the above experimental results, we focus on the conformational dynamics of the prion protein and analyze the effects of the Glu200→Asp and Glu200→Lys point mutations in the HuPrP.

## 2. Materials and methods

### 2.1 Materials

It is worth noting that the wild-type prion protein has a glutamate at 200, and that the Glu200→Asp and Glu200→Lys substitutions occur just before the third helix (a longer, middle helix in Figure 1). An aspartate molecule is an acid, as is glutamate, but the lengths of the side chains are different. In contrast, lysine plays a role as a base, and it is a cationic amino acid at pH 7. The total charges of the models are as follow: models 1 and 2 are “-3” and model 3 is “-1”. The MD simulations have been performed on three model structures of the HuPrP. Model 1 is derived from the NMR structures of HuPrP (125-228) [PDB [23] code: 1QM2, [17]]. The model includes a

globular domain (Figures 1-2), and we called model 1 a "wild-type structure." Models 2 and 3 are mutant structures containing the Glu200→Asp and Glu200→Lys mutations. These two models are built from the NMR structures, by replacing the Glu200 with Asp and Lys, respectively. Glu200→Lys in model 3 is a disease-related amino acid exchange, so we call this model a "mutant type structure."

## 2.2 Molecular dynamics simulations

We have used the program package AMBER5.0 [24] to perform the molecular mechanics potential energy minimizations and MD simulations. The all-atom force field of Cornell et al. [25] was used for all MD simulations. A system was solvated with TIP3P water molecules [26] generated within a rectangular box. The number of solvent water molecules for each system is shown in Table 1. A periodic boundary condition was applied by controlling the pressure. The temperature was kept constant by using the Berendsen algorithm [27] with a coupling time of 0.2 ps. Only bond lengths involving hydrogen atoms are constrained by the SHAKE method [28]. The non-bonded interactions were calculated by a cutoff method. The distance of the cutoff was 14 Å. The integration time step for the MD simulations was 1 fs.

We used the same simulation procedures for all three models under consideration. Firstly, a potential energy minimization was performed on each system. Next, the MD simulations were performed on the energy-minimized states. The whole system temperatures were gradually increased by heating to 300 K for 70 ps and then kept at 300 K for the next 1.6 ns. The trajectories formed at 300 K for 1.6 ns were considered to be the most probable structures under physiological conditions and have been analyzed in detail. The resultant simulations and images of simulated prion proteins were analyzed by using the RasMol [29] and MOLMOL [30] packages.

In this study, we have followed the definition that a hydrogen bond is regarded as being effective, when the distance between the hydrogen atom of the proton donor and the proton acceptor is less than 2.4 Å.

**Table 1.** The number of solvent water molecules for the HuPrP models.

Models of HuPrP	Number of water molecules
Model 1: wild-type prion protein	5112
Model 2: mutant Glu200→Asp prion protein	5102
Model 3: mutant Glu200→Lys prion protein	5182

## 3. Results

### 3.1 RMSD

Figure 3 shows the root-mean-square deviations (RMSD) of the globular domain (125-228) for all three HuPrP models under consideration. The RMSD of the wild-type protein (model 1) was kept at around 2.5 Å for the 1.6 ns simulation, which indicates that the globular domain is stable. The RMSD of the mutant Glu200→Lys protein (model 3) is gradually increased to 2.5 Å from the start of simulation and then it fluctuates in the region of 4-5 Å after about 0.8 ns. Thus, in the mutant Glu200→Lys protein, the essential conformational changes seem to occur after 0.8 ns, when the RMSD is considerably increased. With regard to model 2 (Glu200→Asp substitution), the

RMSD possesses a nontrivial behavior: it increases up to the value of 5 Å at the start of simulation and then it decreases to 2.5 Å after the point of 0.6 ns.

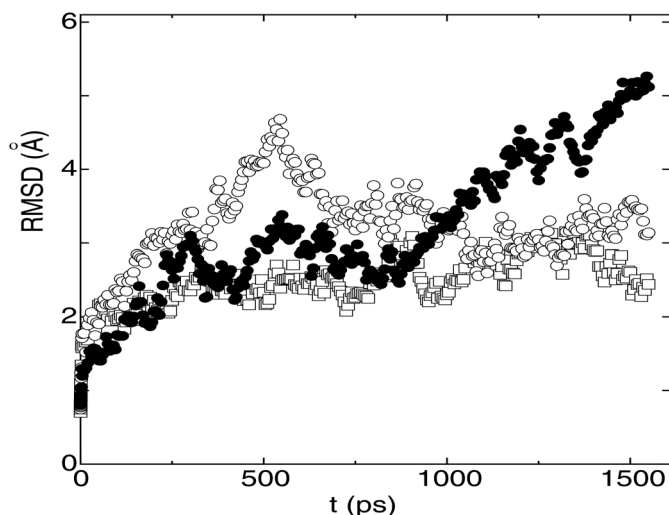


**Figure 3.** The RMSD (Root-Mean-Square-Deviations) (Å) as a function of time (ps) for the wild-type (white marks) and the mutant proteins (white circles: Glu200→Asp; black circles: Glu200→Lys).

### 3.2 MD simulation structures

The final structural images of the MD-simulations for the three models are shown in Figure 4. This figure indicates that the globular domain of the wild-type prion is stably maintained throughout the whole simulation period. For the mutant Glu200→Lys protein (model 3) we observe a partially structural rearrangement: the third (longest)  $\alpha$ -helix H3 is destroyed at residue 219. H3 is reorganized to interact with a strand between H1 and S1. The comparison of models 1 and 3 clearly shows that the  $\alpha$ -helix H1 for model 3 approaches very close to H3. In addition, H3 interacts with the strand between H1 and S1 by forming a new hydrogen bond. Thus, the interaction between H1 and H3 seems to result in the protein's structural rearrangement (see Figure 4, left and right).

The middle picture in Figure 4 shows the final configuration for model 2 (mutant Glu200→Asp prion). The initial structural changes in model 2 look almost the same as those in model 3. We have

compared the MD-simulation structures of models 2 and 3 at 0.6 ns (the data are not shown). The longest  $\alpha$ -helix H3 begins to bend at residue point 219, in the same way as in model 3. The structure will not collapse completely, however; as seen from Figure 4 (middle), the protein will be properly refolded.

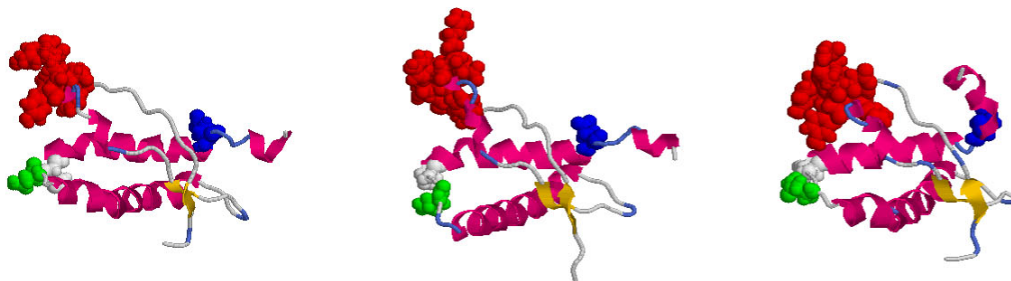


**Figure 4.** The structure plots of the HuPrP models for the final state (1.6 ns) (left: model 1 (wild- type prion protein), middle: model 2 (mutant Glu200→Asp protein), and right: model 3 (mutant Glu200→Lys protein)). In these figures, the  $\alpha$ -helices H2 and H3 are represented by pink ribbons, the atomic positions of the amino acid residues (numbered 141-149) for  $\alpha$ -helix H1 are shown in red. Also the atomic positions of the residues 200 (white), 197 (green), and 219 (blue) are shown for the better understanding of conformational changes in the systems.

### 3.5 Hydrogen bond network maps

In this section, we investigate formation of the hydrogen bond network in the mutant Glu200→Lys prion in detail. The results of previous sections indicate that structural conformations in the prion protein seem to be strongly attributed on the Glu200→Lys amino acid replacement. We have divided the whole protein's structure into three regions (numbered 1, 2, and 3 in Figures 5- to 7), to better understand hydrogen bond formation. In the initial state (Figure 5), we have found just one hydrogen bond at around the mutation point Lys200, which exists between residues Thr199 and Asp202 (see region 3), and two hydrogen bonds, involving residues Ala133 and Arg220 (region 2). With regard to the final state (Figures 6 and 7), we found several new hydrogen bonds, which are formed in response to the Glu200→Lys substitution. In region 1, the new hydrogen bonds are formed between Asp202 and Tyr149 (Asp202- Tyr149) and between Arg208 and Glu146 (Arg208-Glu146). The latter contains two hydrogen bonds. In region 2, we have found a new hydrogen bond within Ser132-Arg220, the side chains of which are exposed to solvent. Two hydrogen bonds involving Ala133-Arg220, which are observed in the initial state, are now transformed into a single bond. In region 3, there are no essential changes between the initial and final states. It is worth noting that there are also no new hydrogen bonds, that might involve the mutation at 200 directly. The residue at 200 is the first in the  $\alpha$ -helix H3, and it doesn't form any interaction with the other parts of the protein. In contrast, the presence of the Lys200 (instead of the Glu200) essentially changes the total hydrogen bond network and causes a partially unfolded conformation.

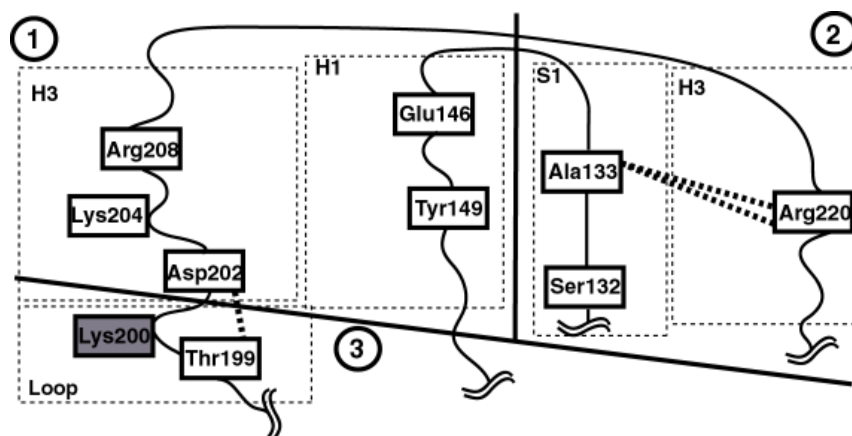


**Figure 5.** A hydrogen bond network map for model 3 (mutant Glu200→Lys prion protein) at the initial state.

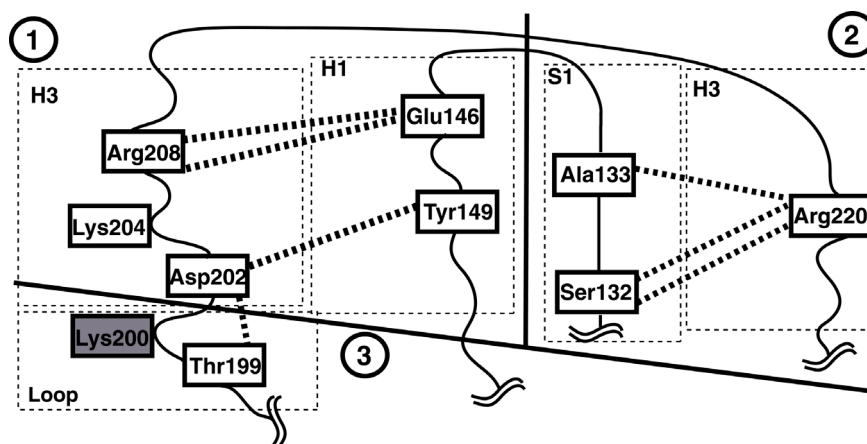


**Figure 6.** A hydrogen bond network map for model 3 (mutant Glu200→Lys prion protein) at the final state, 1.6 ns.

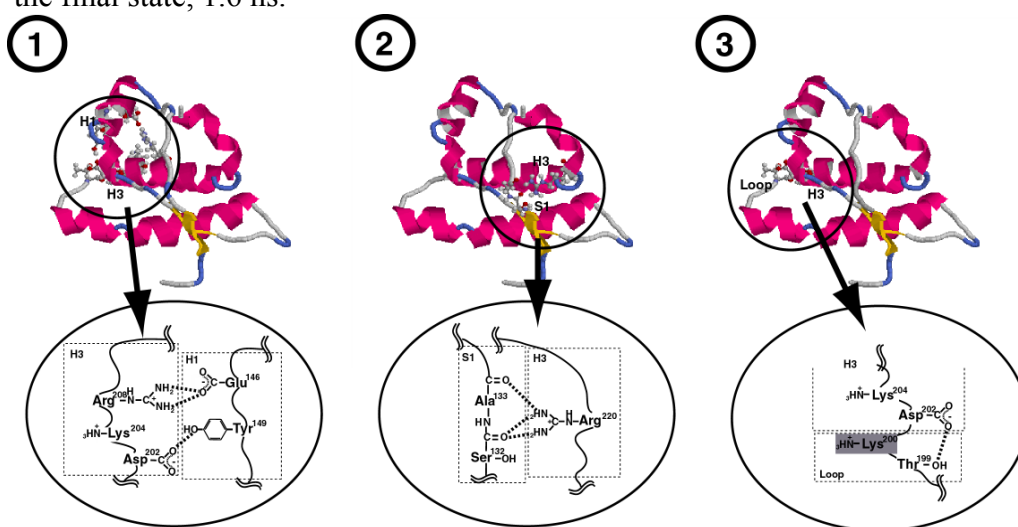


**Figure 7.** A schematic diagram of the hydrogen bond network, for the same regions as in Figure 5 (mutant Glu200→Lys prion protein), for the final state, 1.6 ns.

## 4. Discussion

In our current work, we have performed MD simulations on human prion proteins to study the effect on the structural conformations of the individual amino acid substitutions at the residue point 200. We examined three prion models, the wild type (model 1) and two mutant structures (model 2: Glu200→Asp; and model 3: Glu200→Lys). The Glu200→Lys mutation is found in a well-known type of genetic CJD, while the Glu200→Asp has been identified as being related to CJD. Our simulation results reveal that models 1 and 2 maintain the native protein structure, whereas model 3 partially unfolds. These findings have been proven on the basis of the RMSD, the hydrogen bond network, and other simulation data. Firstly, the RMSD of models 1 and 2 shows that it remains constant at around the value of 2.5 Å. This indicates that the globular domains are reasonably stable over a long simulation time [33][34]. The RMSD in model 3 gradually increases up to the value of 4-5 Å at 0.8 ns from the start of simulation. Secondly, the prion protein's structural images in all three models have been analyzed and compared. In model 3, the prion structure partially unfolds at the middle of the third  $\alpha$ -helix H3. The H3 rearranges to interact with the strand between H1 and S1. Thirdly, for the mutant Glu200→Lys prion, we observed a new hydrogen bond network (within the Asp202-Tyr149, Arg208-Glu146, and Ser132-Arg220 regions).

Recently some experimental data on the Glu200→Lys mutation have been reported. Swietnicki et al. [36] studied the thermodynamic stability of the human prion protein, and suggested that the E200K mutation (Glu200→Lys) induces very little destabilization of the prion structure. Zhang et al. [37] have determined the structure of the CJD-related E200K variant in solution by multi-dimensional NMR spectroscopy. Their opinion is that the backbone structures of the wild-type and E200K prion are not so different. The E200K mutation causes just a different surface electrostatic potential and a loss of the salt-bridge interaction (which is observed in the wild-type structure). This disappearance of the salt-bridge interaction is in good agreement with our simulation (see Figures 5 to -7). In our opinion, the partially unfolded structure appearing in model 3 could be one of the local energy-minimum states and/or an intermediate in the conversion mechanism from PrP<sup>C</sup> to PrP<sup>SC</sup>. Our simulation results also are in good agreement with some experimental data regarding the mobility of the  $\alpha$ -helix H1 [20][21][22]. In addition to these results, our other interest was that the Glu200→Asp prion behaves in a similar manner as does model 1, even though the length of its side chain is shorter than that of the wild-type protein. From the simulation data on these three prion models, we conclude that residue 200 could maintain the balance of the relative positions among the three  $\alpha$ -helices, by simultaneously interacting with the solvent and the solute. Namely, the aspartate amino acid can act as a substitute for the glutamate, but the lysine substitute might not work properly to keep such a relative balance. Thus, the presence of the lysine at the mutation point brings conformational instability and partial unfolding. In summary, the prion structure has to be very sensitive with respect to the type of the amino acid replacement at the residue point 200.

## References

- [1] A. Aguzzi, C. Weissmann, *Nature*, **389**, 795-812 (1997).
- [2] R. G. Wills, J. W. Ironside, M. Zeidler, et al., *Lancet*, **347**, 921-925 (1996).
- [3] J. S. Griffith, *Nature*, **215**, 1043-1044 (1967).
- [4] S. B. Prusiner, *Annu. Rev. Microbiol.*, **43**, 345-374 (1989).



- [5] C. Weissmann, M. Fischer, A. Raeber, H. Beler, A. Sailer, D. Shmerling, T. Rulicke, S. Brandner, A. Aguzzi, *Cold Spring Harbor Symp. Quant. Biol.*, **61**, 511-522 (1996).
- [6] S. B. Prusiner, *Trends Biochem. Sci.*, **21**, 482-487 (1996).
- [7] N. Stahl, M. A. Baldwin, D. B. Teplow, L. Hood, B. W. Gibson, A. L. Burlingame, S. B. Prusiner, *Biochem.* **32**, 1991-2002 (1993).
- [8] K. M. Pan, M. Baldwin, J. Nguyen, M. Gasset, A. Seban, D. Groth, I. Mehlehorn, Z. Huang, R. J. Fletterick, F. E. Cohen, S. B. Prusiner, *Proc. Nat. Acad. Sci. USA.*, **90**, 10962-10966 (1993).
- [9] J. Safar, P. P. Roller, D. C. Gajdusek, C. J. Gibbs, *Protein Sci.*, **2**, 2206-2216 (1993).
- [10] D. G. Donne, J. H. Viles, D. Groth, I. Mehlhorn, T. L. James, F. E. Cohen, S. B. Prusiner, P. E. Wright, H. J. Dyson, *Proc. Natl. Acad. Sci. USA*, **94**, 13452-13457 (1997).
- [11] R. Riek, S. Hornemann, G. Wider, R. Glockshuber, K. Wuthrich, *FEBS Letter*, **413**, 282-288 (1997).
- [12] R. Riek, S. Hornemann, G. Wider, M. Billeter, R. Glockshuber, K. Wuthrich, *Nature*, **382**, 180-182 (1996).
- [13] R. Riek, G. Wider, M. Billeter, S. Hornemann, R. Glockshuber, K. Wuthrich, *Proc. Natl. Acad. Sci. USA*, **95**, 11667-11672 (1998).
- [14] H. Liu, S. Farr-Jones, N. B. Ulyanov, M. Llinas, S. Marqusee, D. Groth, F. E. Cohen, S. B. Prusiner, T. L. James, *Biochem.*, **38**, 5362-5377 (1999).
- [15] T. L. James, H. Liu, N. B. Ulyanov, S. Farr-Jones, H. Zhang, D. G. Donne, K. Kaneko, D. Groth, I. Mehlhorn, S. B. Prusiner, F. E. Cohen, *Proc. Natl. Acad. Sci. USA.*, **94**, 10086-10091 (1997).
- [16] L. F. Garcia, R. Zahn, R. Riek, K. Wuthrich, *Proc. Natl. Acad. Sci. USA.*, **97**, 8334-8339 (2000).
- [17] R. Zahn, A. Liu, T. Luhrs, R. Riek, C. V. Schroetter, L. F. Garcia, M. Billeter, L. Calzolari, G. Wide, K. Wuthrich, *Proc. Natl. Acad. Sci. USA.*, **97**, 145-150 (2000).
- [18] S. Liemann, R. Glockshuber. *Biochem.*, **38**, 3258-3267 (1999).
- [19] D. Shmerling, I. Hegyi, M. Fischer, T. Blattler, S. Brandner, J. Gotz, T. Rulicke, E. Flechsig, A. Cozzio, C. von Mering, C. Hangartner, A. Aguzzi, C. Weissmann, *Cell.*, **93**, 203-214 (1998).
- [20] M. P. Morrissey, E. I. Shakhnovich, *Proc. Natl. Acad. Sci. U.S.A.*, **96**, 11293-11298 (1996).
- [21] E. Hanan, O. Goren, M. Eshkenazy, B. Solomon, *Biochem. Biophys. Res. Commun.*, **280**, 115-120 (2001).
- [22] C. Korth, B. Stierli, P. Streit, M. Moser, O. Schaller, R. Fischer, W. Schulz-Schaeffer, H. Kretzschmar, A. Raeber, U. Braun, F. Ehrensperger, S. Hornemann, R. Glockshuber, R. Riek, M. Billeter, K. Wuthrich, B. Oesch, *Nature.*, **390**, 74-77 (1997).
- [23] H. M. Berman, J. Westbrook, Z. Feng, G. Gilliland, T. N. Bhat, H. Weissig, I. N. Shindyalov, P. E. Bourne, The Protein Data Bank, *Nucleic Acids Res.*, **28**, 235-242 (2000).
- [24] D. A. Case, D. A. Pearlman, J. W. Caldwell, T. E. Cheatham III, W. S. Ross, C. L. Simmerling, T. A. Darden, K. M. Merz, R. V. Stanton, A. L. Cheng, J. J. Vincent, M. Crowley, D. M. Ferguson, R. J. Radmer, G. L. Seibel, U. C. Singh, P. K. Weiner, P. A. Kollman, AMBER 5., University of California (1997).
- [25] W. D. Cornell, P. Cieplak, C. I. Bayly, I. R. Gould, K. M. Merz Jr., D. M. Ferguson, D. C. Spellmeyer, T. Fox, J. W. Caldwell, P. A. Kollman, *J. Am. Chem. Soc.*, **117**, 5179-5197 (1995).
- [26] W. L. Jorgensen, J. Chandrasekhar, J. D. Madura, *J. Chem. Phys.*, **79**, 926-935 (1983).
- [27] H. J. C. Berendsen, J. P. M. Postma, W. F. van Gunsteren, A. DiNola and J. R. Haak, *J. Chem. Phys.*, **81**, 3684-3690 (1984).
- [28] J. P. Ryckaert, G. Ciccotti, H. J. C. Berendsen, *J. Comput. Phys.*, **23**, 327-341 (1997).
- [29] R. A. Sayle, E. J. Milner-White, *Trends in Biochem. Sci.*, **20**, 374-376 (1995).
- [30] R. Koradi, M. Billeter, K. Wuthrich, *J Mol. Graphics*, **4**, 51-55 (1996).

- [31] O. G. Parchment, J. W. Essex, *Proteins: Struct. Funct. Genet.*, **38**, 327-340 (2000).
- [32] N. Okimoto, K. Yamanaka, A. Suenaga, M. Hata, T. Hoshino, *Biophys. J.*, **82**, 2746-2757 (2002).
- [33] K. Kholmurodov, N. Okimoto, Y. Hirano, T. Ebisuzaki, *RIKEN Review*, **48**, 16-18 (2002).
- [34] K. Kholmurodov, N. Okimoto, Y. Hirano, T. Ebisuzaki, The Meeting Abstracts of the 16<sup>th</sup> Molecular Simulation Society of Japan, Niigata., **127L** (2002).
- [35] M. Billeter, K. Wuthrich, *Archiv of Virol.*, **16**, 251-263 (2000).
- [36] W. Swietnicki, R. B. Petersen, P. Gambetti, W. K. Surewicz, *J. Biol. Chem.*, **47**, 31048-31052 (1998).
- [37] Y. Zhang, W. Swietnicki, M. G. Zagorski, W. K. Surewicz, F. D. Sonnichsen, *J. Biol. Chem.*, **43**, 33650-33654 (2000).